

Chaotic dynamics of cold atoms in multidimensional optical lattices

Sergey V. Prants

Received: 22 May 2024 / Published online: 12 February 2025

© The Author(s), under exclusive licence to Springer Nature Switzerland AG 2025

Abstract

Optical lattices, created by interfering laser beams, are efficient tools to manipulate cold atoms by adjusting the lattice geometry and parameters. A number of dynamical effects has been studied with cold atoms in one-dimensional optical lattices in classical, quantum, and semiclassical regimes. Recently, it has been shown that multi-dimensional optical lattices may lead to deeply different dynamics of non-interacting atoms allowing us to investigate the quantum–classical correspondence. We discuss the recent progress in studying classical, semiclassical, and quantum chaotic dynamics of cold atoms in two-dimensional and three-dimensional optical lattices with non-trivial geometry. The special attention is paid to classical versus quantum dynamics of atoms with the coupling between the internal and translational degrees of freedom. The dynamical mechanisms of transition to chaos and inhibition of the onset of chaos for atoms trapped inside wells of the optical potential and moving between different wells are discussed. We propose the experimental schemes that could distinguish between the regular and chaotic dynamics. The perspectives for observation of quantum chaos with cold atoms, that is the quantum regime of a system, whose classical dynamics is chaotic, are considered.

Keywords Dynamical chaos · Cold atoms · Two-dimensional and three-dimensional optical lattices

Introduction

Optical lattices (OLs) are created by interfering laser beams, generally, in three mutually orthogonal directions. If atoms are illuminated by light, the electric component of the laser field induces a dipole moment interacting with the electric field. This modifies the energy of the internal states of atoms in a way that depends both on the light intensity and frequency. Atoms in a standing wave experience the action of the light-induced force [1, 2] that induces a periodic potential energy landscape. OLs have been widely used as a way to cool, trap, and control atomic motion; see, e.g., [3–9]. The OLs with the dimension from 3D to 0D and various geometry have been experimentally implemented; see, e.g., [10–12], by adjusting the number of laser beams, modifying the interference angle between the beams and phase to control the lattice spacing, and by varying the laser frequency and intensity to control the OL depth.

Well-isolated cold atoms loaded in OL are ideal candidates for quantum information processors and for the investigation of nonlinear phenomena, including classical, semiclassical, and quantum chaos. As to terminology used in this paper, classical chaos means chaotic dynamics, in the case where atoms can be considered as classical point-like objects without internal structure. Semiclassical chaos means the conditions, under which the translational degree of freedom can still be considered as classical, but the internal structure is quantum-mechanically treated or vice versa. Quantum chaos means manifestations of some features of classical chaos in the regime, where both the external and internal degrees of freedom are quantized.



A number of chaotic effects with cold atoms in 1D OLs has been experimentally studied, including ballistic motion, oscillations in wells of the optical potential, Brownian motion, anomalous diffusion, and Lévy flights; see, e.g., [13–16]. Since the atoms in 1D OLs are not transversely confined, the experiments are restricted to microsecond time scale, before the atoms quit the beam. Majority of the experimental and theoretical works have been carried out far away from the optical resonance, where spontaneous emission could be suppressed. By adjusting the detuning between the laser and atomic transition frequencies, it is possible to regulate the spontaneous rate and the depth and sign of the effective optical potential affecting the atoms. However, to observe manifestations of chaotic effects in far-detuned 1D OLs, one should work with (quasi)periodically perturbed OLs.

If one works near the resonance, chaotic effects may arise without any modulation of 1D OLs, i.e., in a rigid OL, as it has been shown theoretically in a number of papers by the author with coworkers. This becomes possible due to interaction of the internal and external atomic degrees of freedom. A number of dynamical effects has been found and studied including chaotic Rabi oscillations [17, 18], chaotic scattering of atoms and dynamic fractals [19, 20], and a class of Lévy flights [15, 19, 21, 22]. Detailed theories of Hamiltonian and dissipative chaotic transport of cold atoms in rigid 1D OLs have been elaborated in Refs. [23] and [24], respectively. A review on quantum chaos and quantum–classical correspondence with cold atoms can be found in [25]. The effects proposed can be used in some practical issues, for example, in optical nanolithography to create the high-resolution atomic spatial structures on substrates below the diffraction limit [26] and to create a light-induced atomic elevator [27] in order to lift cold atoms against gravity.

The paper is organized as follows.

In Sec. 2, the works on chaos with classical atoms in 2D and 3D OLs are briefly discussed. In Sec. 3, we focus on semiclassical chaos with coupled translational and internal degrees of freedom of atoms. Section 4 contains some speculations on the perspectives of observation and description of quantum chaos with cold atoms in 2D and 3D OLs. A comprehensive list of references concludes the paper.

Classical chaos in optical lattices

Atom in a standing wave undergoes the force with the potential $U \propto I/\Delta$, where Δ is the detuning between the laser and atomic transition frequencies. Spontaneous emission of atoms is proportional to I/Δ^2 . If Δ is sufficiently large, we can neglect the spontaneous emission and exclude the internal dynamics of atoms from the consideration adiabatically. In order to observe some chaos-like effects, it is necessary to add a periodic or quasi-periodic external forcing. This simplifies analysis and experimental implementation, but prevents the appearance of some interesting dynamical effects. Working near the resonance, chaotic motion of cold atoms and signatures of chaos in the Rabi oscillations may appear in a 1D OL without any modulation. The classical or quantum nature of atoms in OLs depends on the ratio between the energy of the atoms and the depth of the OL wells. If the wells are deep as compared with the atomic energy, the atoms can be considered as classical point-like objects [28]. The underlying physics in majority of investigations is that of a single atom, without any interaction between atoms. The collection of atoms simply increases the observable signal. The quantum properties of cold atoms in the context of quantum chaos have been considered only for the atoms with the internal structure in a 1D OL without external forcing [25] and in periodically-kicked far-detuned 1D OLs; see, e.g., [14, 16].

In this section, we consider briefly the results on classical chaos with point-like atoms in conservative 2D and 3D OLs without internal dynamics [29–34]. This means that these authors have treated and analyzed classical equations of motion for the atomic momentum and coordinates, using the arsenal of methods of classical chaos theory. The authors of [29, 30] have examined the classical dynamics of cold atoms in square OLs obtained with two orthogonal stationary plane waves. They have studied the dynamics of atoms trapped inside individual

wells of the optical potential and for atoms traveling between the wells. The coupling between two external degrees of freedom of atom leads to chaotic motion in a 2D OL with a square mesh.

Atoms with the energy $H < H_T$ are trapped in a well, because they cannot overcome the barrier. Here, H_T is the value of the potential energy at the saddle point of the intensity. The behavior of atoms strongly differs on the sign of detuning. For the blue detunings ($\Delta > 0$) and at very small energies, atom moves regularly around the bottom of the well along a quasi-periodic trajectory. If the energy is increased, chaos appears in the vicinity of a separatrix. If the energy is further increased, chaos expands on a Poincaré section with some remaining islands of regular motion. At $H = 1$, chaos dominates within a narrow area with tori remaining around the locked X and Y periodic cycles [29]. It is a typical scenario for emergence of Hamiltonian chaos; see, e.g., [18, 22, 35].

For the red detunings ($\Delta < 0$), phase locking between the motions in X and Y directions is a dominant mode of motion. Chaos appears close to the separatrix at $E \approx 1$, but it remains marginal due to an original degeneracy of frequencies of the coupled pendula and due to strong coupling between them. The regime of motion depends on the values of the energy H and detuning Δ . At $H \leq 1$ and $\Delta > 0$, atom remains in a single well of the optical potential. If atom has the energy larger than the potential maximum, i.e., at $H > 4$, its trajectory is purely ballistic. In the intermediate case where $1 < H < 4$, the atom can visit a large number of wells in a random-like manner; it was earlier shown for atoms in a rigid 1D OL [19, 23].

At $\Delta < 0$, the maximum of the potential is $H = 1.33$, and the atoms with the energy exceeding this value perform ballistic flights, whereas the atoms with $1 < H < 1.33$ exhibit chaotic walking between the wells [29].

The authors of [29] proposed a way to differ the atomic behavior in red and blue OLs based on measuring of the time, when ballistic atoms will reach the edge of the OL, and finally leave it. This simple measure of the “lifetime” of atoms gives information about trapped and ballistic atoms. The functions of the number of atoms leaving the lattice versus time are quite different in blue and red OLs; see Fig. 6 in [29] demonstrating the existence of several characteristic times at a decrease of the number of atoms. These results provide qualitative and quantitative information about the nature of the dynamics of atoms. Therefore, the measure of the lifetime of atoms appears to be a signature of the chaotic dynamics of atoms in 2D OLs.

In a series of papers, L. Reichl with co-workers [31–34] have considered chaotic dynamics of cold atoms confined to far-detuned 2D and 3D OLs without internal structure. They focused on detailed analysis of the classical nonlinear dynamics of a dilute gas of atoms for different polarization of the laser beams and on finding the mechanisms leading to the onset of chaos. Under these conditions, chaos cannot arise in the absence of interference between the laser beams propagating in orthogonal directions. Without the interference, the atomic dynamics is integrable and equivalent of two uncoupled pendula. The stable and unstable invariant manifolds of the associated saddle fixed point form a separatrix that is a barrier for mixing. Adjusting the polarization directions and relative phase of the laser beams, it is possible to create conditions for onset of chaos. It has been shown both for 2D [31, 33, 34] and 3D OLs [32] that chaos occurs after a bifurcation at the saddle point that leads to splitting and transversal intersections of stable and unstable invariant manifolds. With increasing energy, this bifurcation gives rise to a growing chaotic sea in the neighborhood of the broken separatrix with remaining islands of regular motion. It is again a typical scenario for the onset of dynamical chaos in Hamiltonian systems [35].

Stochastic layers of different resonances in the phase space may intersect to form a web in Hamiltonian nonlinear dynamical systems with the number of degrees of freedom greater than two. A single trajectory can diffuse throughout the web from one resonance to the other, even if the disturbance is small. This phenomenon is called Arnold diffusion [36] and has been investigated for a variety of objects, from atoms to the solar system. In Ref. [34], the authors treated Arnold diffusion in the classical dynamics of the center-of-mass motion of noninteracting two-level atoms in a 2D OL with a time-periodic amplitude modulation. Such OLs have been experimentally realized; see, e.g., [10]. With increasing perturbation amplitude, the width of nonlinear resonances increases, and the resonances begin to overlap, as it has been established by Chirikov [37], until the

system reaches the so-called “Chirikov regime.” Chaotic regions in the phase space become global, and random diffusion dominates the dynamics.

Semiclassical chaos in optical lattices

The next step has been done in Refs. [38, 39], where coherent dynamics of cold atoms in 2D OLs with interfering and non-interfering laser beams has been studied under the conditions close to the optical resonance. Different regimes of translational motion of atoms and their dependence on the internal degrees of freedom have been found and described. Possible experiments have been proposed and designed [39] in order to observe some manifestations of deterministic chaos.

A simple 3D OL can be formed by the electric field

$$\mathcal{E}(X, Y, Z) = \mathcal{E}_0[\cos(k_f X) + \cos(k_f Y) + \cos(k_f Z)]$$

with the help of six counter-propagating laser beams along X , Y , and Z axes with the same frequencies ω_f , wave vectors k_f , and amplitudes \mathcal{E}_0 . In the absence of interference between the laser beams, the optical potential is given by a simple formula

$$V = -V_0[\cos^2(k_f X) + \cos^2(k_f Y) + \cos^2(k_f Z)].$$

In the semiclassical approximation and in the frame rotating with the laser frequency ω_f , the Hamiltonian of a two-level atom has the form

$$\hat{H} = \left[\frac{1}{2m_a}(p_x^2 + p_y^2 + p_z^2) + \frac{1}{2}\hbar(\omega_a - \omega_f)\hat{\sigma}_w - \hbar\Omega(\hat{\sigma}_- + \hat{\sigma}_+)(\cos k_f x + \cos k_f y + \cos k_f z) \right], \quad (1)$$

where $\hat{\sigma}_{\pm, w}$ are the Pauli operators, $x \equiv k_f X$, $y \equiv k_f Y$, $z \equiv k_f Z$ and $p_x \equiv P_X/\hbar k_f$, $p_y \equiv P_Y/\hbar k_f$, $p_z \equiv P_Z/\hbar k_f$ are the normalized classical positions and momenta, and $\Omega = d\mathcal{E}_0/\hbar$ is the maximum value of the Rabi frequency, which depends on the electric dipole matrix element d and the amplitude of electric field strength \mathcal{E} .

After normalizing the electric-field strength to its amplitude value, we obtain

$$E(x, y, z) = -(\cos x + \cos y + \cos z).$$

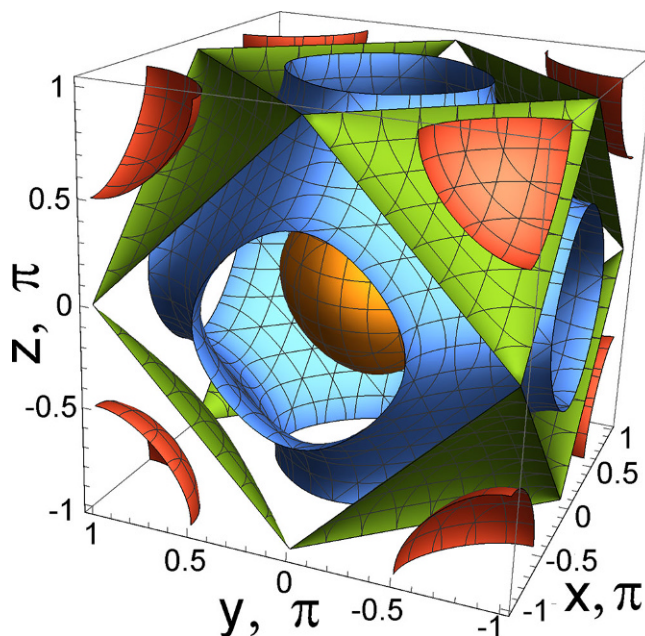
The zeros of this function are distributed on the isosurfaces shown in Fig. 1 for $E = -2$, $E = 0$, $E = 1$, and $E = 2$. At $E = 0$, the zeros are distributed on the nodal surface of a jar-like object with four symmetric hollows in the unit cell of the 3D standing wave composed of three orthogonal 1D standing waves.

The coherent evolution of the atom is described by the set of Hamilton–Bloch equations [40]

$$\begin{aligned} \dot{x} &= \omega_r p_x, & \dot{y} &= \omega_r p_y, & \dot{z} &= \omega_r p_z, \\ \dot{p}_x &= -u \sin x, & \dot{p}_y &= -u \sin y, & \dot{p}_z &= -u \sin z, & \dot{u} &= \Delta v, \\ \dot{v} &= -\Delta u + 2w(\cos x + \cos y + \cos z), & \dot{w} &= -2v(\cos x + \cos y + \cos z), \end{aligned} \quad (2)$$

where u and v are components of the atomic electric dipole moment, w is the population inversion, and dot denotes differentiation with respect to the dimensionless time $\tau \equiv \Omega t$. The nonlinear equations (2) have two control parameters, the normalized recoil frequency $\omega_r \equiv \hbar k_f^2/m_a \Omega$, quantifying the recoil energy the atom

Fig. 1 The isosurfaces of the total electric-field strength $E(x, y, z) = -(\cos x + \cos y + \cos z) = 0$ with $E = -2$ (orange), $E = 0$ (blue), $E = 1$ (green), and $E = 2$ (red)



acquires after stimulated emission and absorption of photons, and the atom–field detuning $\Delta \equiv (\omega_f - \omega_a)/\Omega$. They have two integrals of motion, the length of the Bloch vector $u^2 + v^2 + w^2 = 1$, and the total energy [41]

$$H \equiv \frac{\omega_r}{2}(p_x^2 + p_y^2 + p_z^2) - u(\cos x + \cos y + \cos z) - \frac{\Delta}{2}w = K + I + W, \tag{3}$$

which consists of the kinetic energy $K \equiv \frac{\omega_r}{2}(p_x^2 + p_y^2 + p_z^2)$, optical potential $I \equiv u(\cos x + \cos y + \cos z)$, and the internal energy $W \equiv \frac{\Delta}{2}w$, where $I + W$ is the interaction energy of the atom with the laser fields.

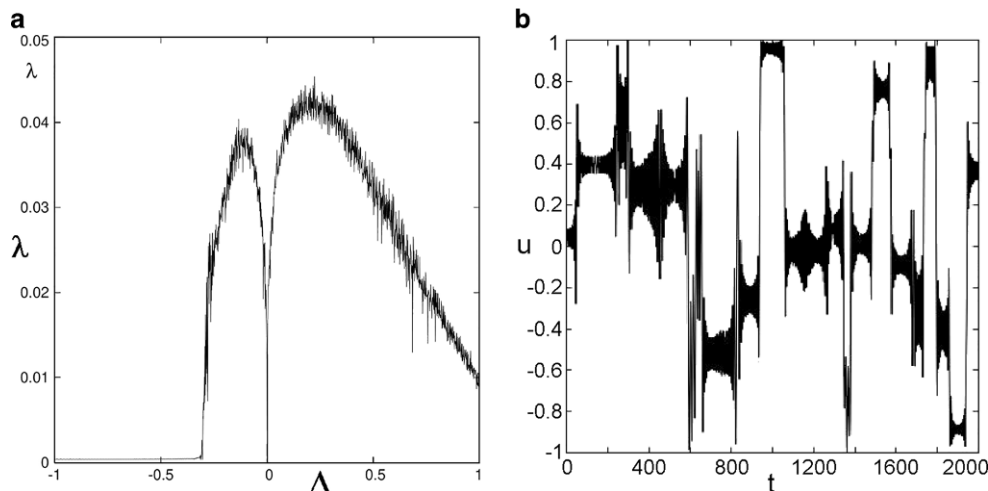
At zero detuning $\Delta = 0$, Eqs. (2) have only regular solutions with zero value of the maximum finite-time Lyapunov exponent λ characterizing the average speed of divergence of initially close by trajectories in the phase space. At $1/|\Delta| \ll 1$, these equations have slow and fast variables. Averaging over the fast temporal scale of the order of $1/|\Delta|$, the kinetic energy of atom becomes a leading term in the averaged dynamics, that is expected to be regular. The Lyapunov exponent has been calculated in dependence on the detuning at fixed values of the recoil frequency $\omega_r = 10^{-3}$ [40, 41]. The result is shown in Fig. 2a. Positive values of λ lie in a narrow range of Δ values on both sides of zero. Therefore, chaotic dynamics may occur at blue and red detunings regardless of the values of the recoil frequency.

Analyzing the total atom energy (3), it has been shown in [40] that there exist three possible regimes of translational motion in a 3D OL, namely, trapping mode at $H < 0$, ballistic mode at $H > 3$, and a wandering mode at $0 < H < 3$, in which atom moves in a random-like way with $\lambda > 0$, being intermitting trappings in wells of the optical potential with flights over its hills.

The light-induced force may change as the atom moves in a periodic OL, especially when atom approaches the nodal surface of the standing wave; see Fig. 1, where the electric field strength E is zero. These changes occur due to behavior of the component of the Bloch vector u ; see Fig. 2b. This quantity experiences abrupt changes, when the atom approaches the nodal surface. The “jumps” in the behavior of u lead to changes in the value of the optical potential $I \equiv u(\tau)E(x, y)$, which, in turn, leads to changes in the kinetic energy and momentum of the atom, because the internal energy $W \equiv \frac{\Delta}{2}z(\tau)$ is relatively small at small detuning values.

The jumps occur when the atom crosses nodal surfaces of E , because u is synchronized with the electric field component of the induced atomic dipole moment. The direct calculation shows [39] that majority of the jumps

Fig. 2 Dependence of the finite-time Lyapunov exponent λ on the atom–field detuning Δ (a) and the component of the atomic electric dipole moment u versus time in the chaotic regime of motion (b). Here, $\Delta = 0.25$, $\lambda \simeq 0.025$, and $\omega_r = 10^{-3}$

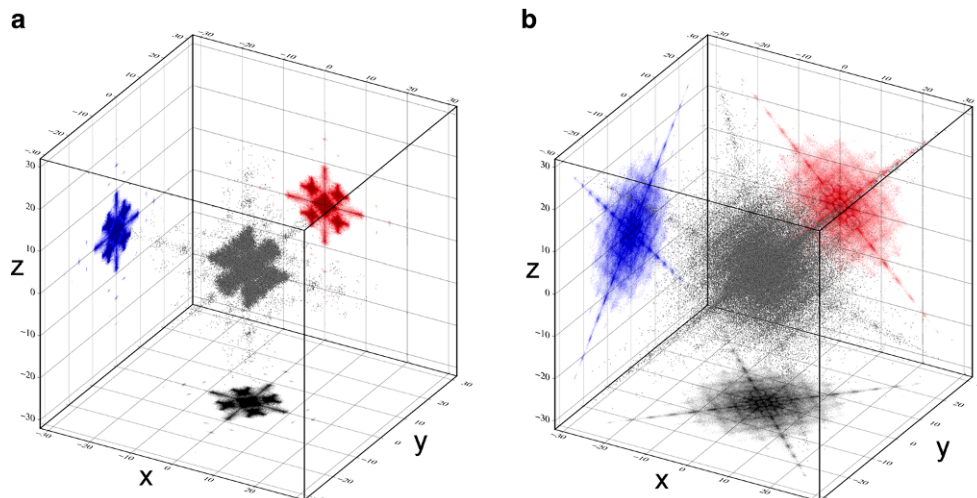


occur when the atom appears near a nodal surface. In this case, u does not necessarily reach zero. Moreover, the jump amplitude is a pseudo-random quantity and can be comparatively small; see Fig. 2b. In any case, the fundamental reason for the chaotic wandering of an atom in absolutely deterministic OLs is a random-like behavior of the component of the Bloch vector u near the nodal surface of a standing light wave. Thus, the interaction of internal and external degrees of freedom under certain conditions generates chaos both in translational motion of atoms and in the Rabi oscillations.

To find some manifestations of chaotic dynamics in a real experiment, numerical experiments have been carried out in [39, 41] with a sufficiently large number of atoms. The idea was to compare spatial distribution of a cloud of atoms for two values of the detuning, one at a value of Δ at which $\lambda = 0$, and the other at a slightly different value of Δ at which $\lambda > 0$. The result is shown in Fig. 3. At $\Delta = -0.5$ with $\lambda = 0$; see Fig. 2a, the majority of atoms are trapped inside the first few cells of the OL around the origin; see Fig. 3a. The density of atoms is maximum inside the cells and minimum in between, being separated by the nodal surfaces of E ; see Fig. 1a.

The distribution is cardinally different in the chaotic mode of motion at $\Delta = 0.25$ with $\lambda \approx 0.025$; see Fig. 2a. The distribution of atoms is irregular inside the cells around the origin due to chaotic motion, although the detuning is blue. The atomic transport, in this mode, is also characterized by long ballistic flights, which looks like long symmetric rays in Fig. 3b.

Fig. 3 Distribution of $N = 10^5$ cold atoms at $\tau = 10^3$ in the regular mode of motion at the red detuning $\Delta = -0.5$ and $\omega_r = 10^{-3}$ (a). Here, projections of the 3D distribution to the planes $x - y$, x, z , and y, z are shown. The same but in the chaotic regime at $\Delta = 0.25$ with $\lambda \approx 0.025$ (b)



Spontaneous emission interrupts coherent evolution at random time moments and causes sudden jumps of the u values to zero, which occur between jumps of u caused by crossings or approaching the nodal surfaces. This stochastic-like behavior masks the effect of deterministic chaos. After many events of spontaneous emission during a real experiment, trajectory of any atom differs from the relaxation-free trajectory under the same initial conditions and at the same values of control parameters. However, the distributions of a large number of chaotically moving non-relaxing atoms and randomly walking spontaneously-emitting atoms are not expected to differ significantly, because the contribution of quantum fluctuations is approximately the same for slightly different values of the detuning. Therefore, the observed differences in the distribution of atoms in the regular and chaotic regimes of motion shown in Fig. 3 may be considered as a manifestation of deterministic chaos in a real experiment.

To record the distribution of atoms, various methods can be used, in particular, the absorption imaging technique [42, 43], providing information about the number and spatial parameters of atomic clouds. In this method, the atomic cloud is irradiated with a near-resonant collimated laser beam just after turning off the OL. The atoms scatter photons out of the laser beam, and the atomic shadow cast is recorded by a CCD camera. By scanning the cloud through the optical resonance, the optical density for each pixel and the number of atoms can be calculated from a series of images.

Perspectives in investigations of quantum chaos with cold atoms in optical lattices

In this paper, we consider the classical and semiclassical dynamics of cold atoms in the regime, where the atoms can be considered as point-like objects. It appears that this dynamics can be complex even for simple and fully deterministic systems. The next step in further investigations is to think about the consequences of obtained results in the quantum regime, where the atoms should be considered as matter waves.

Classical and quantum mechanics are quite different in many aspects. Dynamical chaos in classical systems is characterized by an exponential divergency of initially close by trajectories in the continuous phase space, where the states of the system can be arbitrarily close to each other. The trajectory concept is absent in quantum mechanics, where the phase space is not continuous. Moreover, the evolution of an isolated quantum system is unitary, preventing appearance of any chaos in the classical sense. The common opinion [35, 44–46] is that the term “quantum chaos” means manifestations of specific features in the unitary evolution and/or spectra of a quantum system in the same range of the control parameters, where the corresponding classical analogue demonstrates a chaotic behavior.

The problem of quantum chaos is even more profound in physics, because it may be put in a wider context of the wave–ray correspondence. The propagation of waves in different disciplines in physics may be treated in the ray regime, as an approximation. The manifestations of ray (classical) chaos have been found for electromagnetic waves in microwave cavities; see, e.g., [47], and for acoustic waves in the underwater sound channel in the ocean [48]. Despite major efforts, the problem of the quantum–classical and wave/ray correspondence is still far from being fully understood.

Some manifestations and symptoms of classical chaos in 1D OLs have been found for atomic matter waves; see, e.g., the experiments with far-detuned atoms in a δ -kicked OL [13, 16] and the theoretical results with near-resonant atoms in a rigid OL [25, 49]. When the matter waves propagate through a spatially periodic medium, the allowed propagation energies form bands. The waves, with energies lying in the band gaps, cannot propagate. The authors of [32] have numerically studied the impact of quantum dynamics of atoms on 3D OL and showed the effect of chaos on the energy band structure. The band structure appeared to be sensitive to the level of classical chaos experienced by the atoms.

However, the research of quantum chaos with cold atoms in multi-dimensional OLs is still only on the agenda, both theoretically and experimentally. The expected results, in this area, could be used in various practical issues

including atomic nanolithography, trapping, cooling, selective manipulation and control of single atoms, chemical reaction kinetics, and quantum information processing devices.

Funding The work was supported by the State Task at POI FEB RAS No. 124022100072-5.

Data Availability This manuscript has no associated data.

Conflict of interest The authors declare no conflicts of interest.

References

1. P. Lebedew, *Ann Phys* **311**, 433 (1901)
2. G.A. Askaryan, *Sov Phys JETP* **15**, 1088 (1962)
3. S. Chu, *Rev Mod Phys* **70**, 685 (1998)
4. C.N. Cohen-Tannoudji, *Rev Mod Phys* **70**, 707 (1998)
5. W.D. Phillips, *Rev Mod Phys* **70**, 721 (1998)
6. V.S. Letokhov, *JETP Lett* **7**, 272 (1968)
7. V.G. Minogin, V.S. Letokhov, *Laser Light Pressure on Atoms* (Gordon and Breach Science Publishers, New York, 1987)
8. V. Letokhov, *Laser Control of Atoms and Molecules* (Oxford University Press, New York, 2007)
9. A.P. Kazantsev, G.I. Surdutovich, V.P. Yakovlev, *Mechanical Action of Light on Atoms* (World Scientific, Singapore, 1990)
10. A. Hemmerich, D. Schropp Jr., T.W. Hansch, *Phys Rev A* **44**, 1910 (1991)
11. G. Grynberg, C. Robilliard, *Phys Rep* **355**, 335 (2001)
12. G. Raithel, N. Morrow, *Adv At Mol Opt Phys* **53**, 187 (2006)
13. F.L. Moore, J.C. Robinson, C.F. Bharucha, et al., *Phys Rev Lett* **73**, 2974 (1994)
14. M.G. Raizen, *Adv At Mol Opt Phys* **41**, 43 (1999)
15. F. Bardou, J.P. Bouchaud, A. Aspect, C. Cohen-Tannoudji, *Lévy Statistics and Laser Cooling* (Cambridge University Press, Cambridge, 2002)
16. W.K. Hensinger, N.R. Heckenberg, G.J. Milburn, H. Rubinsztein-Dunlop, *J Opt B: Quantum Semiclass Opt* **5**, 83 (2003)
17. L.E. Kon'kov, S.V. Prants, *JETP Lett* **65**, 833 (1997)
18. S.V. Prants, L.E. Kon'kov, I.L. Kirilyuk, *Phys Rev E* **60**, 335 (1999)
19. V.Y. Argonov, S.V. Prants, *J Exp Theor Phys* **96**, 832 (2003)
20. S.V. Prants, M.Y. Uleysky, *Phys Lett A* **309**, 357 (2003)
21. F. Bardou, J.P. Bouchaud, O. Emile, et al., *Phys Rev Lett* **72**, 203 (1994)
22. S.V. Prants, M. Edelman, G.M. Zaslavsky, *Phys Rev E* **66**, 46222 (2002)
23. V.Y. Argonov, S.V. Prants, *Phys Rev A* **75**, 63428 (2007)
24. V.Y. Argonov, S.V. Prants, *Phys Rev A* **78**, 43413 (2008)
25. S.V. Prants, *Phys Scr* **92**, 44002 (2017)
26. V.O. Vitkovsky, S.V. Prants, *Opt Spectrosc* **114**, 52 (2013)
27. S.V. Prants, *JETP Lett* **104**, 749 (2016)
28. M. Greiner, S. Fölling, *Nature* **435**, 736 (2008)
29. D. Hennequin, D. Verkerk, *Phil Trans R Soc A* **368**, 2163 (2010)
30. D. Hennequin, D. Verkerk, *Eur Phys J D* **57**, 95 (2010)
31. E. Horsley, S. Koppell, L. Reichl, *Phys Rev E* **89**, 12917 (2014)
32. Y. Boretz, L.E. Reichl, *Phys Rev E* **91**, 42901 (2015)
33. M.D. Porter, L.E. Reichl, *Phys Rev E* **93**, 12204 (2016)
34. Y. Boretz, L.E. Reichl, *Phys Rev E* **93**, 32214 (2016)
35. G.M. Zaslavsky, *Phys Rep* **80**, 157 (1981)
36. V.I. Arnold, *Sov Math Dokl* **5**, 581 (1964)
37. B. Chirikov, *Phys Rep* **52**, 263 (1979)
38. S.V. Prants, L.E. Kon'kov, *J Russ Laser Res* **40**, 348 (2019)
39. S.V. Prants, *J Exp Theor Phys* **131**, 410 (2020)
40. S.V. Prants, L.E. Kon'kov, A.A. Didov, *J Russ Laser Res* **42**, 558 (2021)
41. S.V. Prants, *J Russ Laser Res* **43**, 18 (2022)
42. C.J. Foot, *Atomic Physics* (Oxford University Press, New York, 2005)
43. G. Reinaudi, T. Lahaye, Z. Wang, D. Guery-Odelin, *Opt Lett* **32**, 3143 (2007)
44. G. Casati, B.V. Chirikov, F.M. Izrailev, J. Ford, *Stochastic Behavior in Classical and Quantum Hamiltonian Systems. Lecture Notes in Physics* (Springer, Berlin, 1979)
45. M. Gutzwiller, *Chaos in Classical and Quantum Mechanics* (Springer, New York, 1990)

46. L.E. Reichl, *The Transition to Chaos in Conservative Classical Systems: Quantum Manifestations* (Springer, New York, 1992)
47. S. Sridhar, *Phys Rev Lett* **67**, 785 (1991)
48. A.L. Virovlyansky, D.V. Makarov, S.V. Prants, *Phys Uspekhi* **55**, 18 (2012)
49. S.V. Prants, *J Exp Theor Phys* **109**, 751 (2009)

Publisher's Note Springer Nature remains neutral with regard to jurisdictional claims in published maps and institutional affiliations.

Springer Nature or its licensor (e.g. a society or other partner) holds exclusive rights to this article under a publishing agreement with the author(s) or other rightsholder(s); author self-archiving of the accepted manuscript version of this article is solely governed by the terms of such publishing agreement and applicable law.

Authors and Affiliations

Sergey V. Prants¹

✉ Sergey V. Prants
prants@poi.dvo.ru

¹ Laboratory of Nonlinear Dynamical Systems, V.I. Il'ichev Pacific Oceanological Institute of the Russian Academy of Sciences, dynalab.poi.dvo.ru, Vladivostok, Russian Federation